Plant Physiology and Biochemistry 212 (2024) 108780

Contents lists available at ScienceDirect

Plant Physiology and Biochemistry

journal homepage: www.elsevier.com/locate/plaphy

The contrasting photosynthesis and growth response of young test species irrigated with electro-chemical modified water

Giuseppe Barion [a], Camilla Canal [a], Anna Panozzo [a,*], Selina Sterup Moore [b], Simone Piotto [a], Teofilo Vamerali [a]

[a] Department of Agronomy Food Natural Resources Animals and the Environment, Padua University, Viale dell'università 16, 35020, Legnaro, Padua, Italy
[b] Department of Agroecology, Aarhus University, Blichers Allè 20, 8830, Tjele, Denmark

ARTICLE INFO

Keywords:
Electron transport rate
Leaf-to-root biomass ratio
Non-photochemical quenching
Oxidation reduction potential
Stomatal conductance
Water vibrational mode

ABSTRACT

The study evaluated the effects of treating irrigation water with a coaxial flow variator (CFV) on the morpho-physiology of pot-cultivated test species, including cucumber (*Cucumis sativus,* CU), lettuce (*Lactuca sativa*, LE), and sorghum (*Sorghum vulgare*, SO), in early stages of growth. CFV caused a lower oxidation reduction potential (ORP), increased pH and flow resistance and inductance. It induced changes in the absorbance characteristics of water in specific spectral regions, likely associated with greater stretching and reduced bending vibrations compared to untreated water. While assimilation rate and photosynthetic efficiency were not significantly affected at 60 days after sowing, treated water increased the stomatal conductance to water vapour *gsw* (+79%) and the electron transport rate *ETR* (+10%) in CU, as well as the non-photochemical quenching *NPQ* (+33%) in SO. Treated water also reduced leaf temperature in all species (−0.86 °C on average). This translated into improved plant biomass (leaves: +34%; roots: +140%) and reduced leaf-to-root biomass ratio (−42%) in SO, allowing both faster aerial growth and soil colonization, which can be exploited to improve plant tolerance against abiotic stresses. In the C3 species CU and LE, plant biomass was instead reduced, although significantly in LE only, while the leaf-to-root biomass ratio was generally enhanced, a result likely profitable in the cultivation of leafy vegetables. This is a preliminary trial on the effects of functionalized water and much remains to be investigated in other physiological processes, plant species, and growth stages for the full exploitation of this water treatment in agronomy.

1. Introduction

Water covers more than 70% of the earth's surface and is naturally present with a salinity ranging from <0.05% in fresh water to 3–5% in salt water (Mecklenburg et al., 2012). H_2O consists of two hydrogen atoms linked via a covalent polar bond to an oxygen atom at a 105° angle. The interacting forces between individual water molecules are referred to as hydrogen bonds. Water plays a fundamental role in most plant physiological processes, from germination where it allows hydrolysis of starch into glucose, to photosynthesis where it acts as an electron donor in the photosystems of the chloroplast to produce DADPH and ATP (Hopkins and Hüner, 2004). The availability of water affects the cell turgor in plant tissues and stimulates stomatal opening, as well as leaf orientation ability. Water is also the mean by which minerals are mobilized, absorbed, and translocated from the soil to the plant (Blatt et al., 2014).

In general, the absorption spectrum of individual compounds is determined by quantum changes in the atomic and molecular energies of the given compound (Wozniak and Dera, 2007; Cooper et al., 2019). Water can establish numerous hydrogen bonds with particularly complex dynamics and strongly absorbs electromagnetic radiation in the infrared region of light. Infrared spectroscopy (IR) is the most sensitive and powerful method for detecting hydrogen bonds, and several absorbance peaks in the infrared and near visible regions have been found to be associated with different abundances of vibrational wave packets of water molecules (Walrafen and Pugh, 2004; Maréchal, 2011; Tennyson et al., 2014). To ensure limited signal intensity and overlap of peaks, analysis of the whole IR region of water is only feasible for very thin samples (Bernath, 2002). It has been demonstrated that water absorbance involves different wavelength regions depending on the abundance of symmetrical and asymmetrical *stretching* and *bending* vibrations (Eisenberg and Kauzmann, 2005). Absorbance at high

* Corresponding author.
E-mail address: anna.panozzo@unipd.it (A. Panozzo).

https://doi.org/10.1016/j.plaphy.2024.108780
Received 22 March 2024; Received in revised form 16 May 2024; Accepted 27 May 2024
Available online 28 May 2024

wavelengths in the infrared region, i.e., between 200 and 660 μm, is generally associated with reticular (mixed) vibrations which coexist in the whole of rotations and oscillations. Different vibrational characteristics of water can be associated with different electromagnetic properties (Ruud et al., 2000) and oxidation reduction potentials (Piatkowski and Bakker, 2011). These can easily be detected with common lab equipment and may impose differing effects on plant physiological processes.

Coaxial flow variators (CFV) change the flow of water from laminar to turbulent by forcing the flow through a spiral-shaped duct made of metals. Its use is being increasingly adopted by farmers in horticultural and viticultural settings to modify the qualitative properties of irrigation water and improve plant growth, wellbeing, and health. However, studies demonstrating and quantifying the effect of such practice on plants have not yet been published. In this framework, the objective of this innovative study was to evaluate: *i*) the changes in electrical and chemical properties of water when forced through a CFV device; and *ii*) whether irrigation water forced through a CFV device has any effects on the morpho-physiology (root and shoot growth, and photosynthetic efficiency) of cucumber (CU), lettuce (LE), and sorghum (SO) grown in greenhouse settings.

2. Material and methods

2.1. Trial set-up

A pot trial was set up in a greenhouse at the University of Padua experimental farm in 2022. Here three plant species, i.e., lettuce (*Lactuca sativa*, LE), sorghum (*Sorgum vulgare*, SO), and cucumber (*Cucumis sativus*, CU) were cultivated in a sand/silty loam substrate (1:1 w/w) for 60 days. Sand was added to the substrate to facilitate recovery of the root system by washing and sieving at the end of the trial. The resulting pot substrate had a pH of 7.75, with a moderate content of N (0.06%), available P (18 mg P_2O_5 kg^{-1}) and exchangeable K (59 mg K_2O kg^{-1}) (Table SI1). The substrate was fertilized with an 8-24-24 NPK ternary mineral fertilizer at a dose of 4.5 g kg^{-1} substrate. Plants were cultivated in 1.2-L cylinder pots following a randomized experimental design with 9 replicates. Three seeds per pot were sown and seedlings were thinned to one plant per pot following emergence. The plants of the three species were watered roughly every two days, with one of two types of water, i.e. treated water (TW) or control water (CW).

2.2. Water characterization

TW was derived from a local artesian well. The TW passed through a coaxial flow variator (CFV) device (patent SI 21511-2003) (Sajovic, 2004) (Fig. SI1), which allows laminar and spiral water flow in an abduction pipeline by forcing the flow through a large spiral-shaped duct made of iron and copper. An oval-shaped curved circular pipe-like enclosure generates such flow types inside the plumbing. In its longitudinal direction, the enclosure holds a spiral-shaped band and a swinging reed-like turbulence focusing device on the internal surface. The enclosure and focusing parts were realized with longitudinal fleeting and non-parallel axes (Sajovic, 2004).

The absorption spectra of TW and CW in the 0,24-1,24 μm region were recorded by a spectrometer (FOSS MilkoScan7 RM, Foss Analitycal – Padua IT) by measuring the absorption coefficient (A.C.) considering the sample thickness (d), as follows:

$$A.C. = \frac{2.303 \times \text{Adsorbance}}{\text{d}}$$

The MilkoScan7 RM here applied to water samples, is commonly used for analyzing milk and a wide variety of liquid and semi-solid dairy products through infrared spectroscopy in the near-infrared (NIR) and mid-infrared (MIR) wavelength regions.

Further electrical characteristics of water, such as pH, Oxidation Reduction Potential (ORP), and amount of dissolved O_2 were measured with a HI9829 Multi parameter electrical probe (Hanna Instrument, Woonsocket, RI – USA). Water flow resistance (R) and inductance (L) were measured by a handheld ELC-131D digital electrical meter (Escort Instruments Corporation, Taipei, Taiwan) connected to the ends of a 2-mm thick 7-cm long solenoid (5 coils with 15-mm diam.) made of copper immersed in the water.

Also the concentration of bicarbonate (HCO_3^-) in the water was measured via titration with HCl and the indicator phenolphthalein, following the method of Rice and Bridgewater (2012).

The electrochemical parameters pH, ORP, R, and L of TW vs. CW water were also monitored at 2- or 3-day intervals over a 12 day period in the lab. The water samples were maintained at ambient 20 °C temperature in closed glass beakers that were opened only for the purpose of measuring said parameters.

During the pot trial, a special syringe equipped with a porous probe (Rhizom MOM, Rhizosphere Research Product, Wageningen – The Netherlands) able to collect pore water from the growing substrate was installed in each pot. At the end of the trial, the content of each syringe was collected; the number of water samples analysed was reduced from 9 (number of pots) to 3. Due to the limited maximum syringe capacity of 10 mL, only some electrical parameters could be measured, i.e., R, L, and pH.

2.3. Plant analyses

Photosynthesis was analysed the day before harvest with a Li-COR 6800 (Li-COR Inc., Lincoln, Nebraska, USA) portable fluorimeter on the last fully developed leaf, i.e., 7th, 9th and 6th in LE, CU and SO, respectively. This equipment is able to measure leaf temperature, photosynthesis efficiency expressed as the ratio between variable and maximum fluorescence (*Fv'/Fm'*), efficiency of electron transport from photosystem II (Electron Transport Rate, *ETR*), energy loss by non-photosynthetic processes (Non-photochemical Quenching, *NPQ*), net CO_2 assimilation (*A*), and the coefficient of stomatal conductance (*gsw*). The temperature of the leaf chamber was maintained at 27 °C, the relative humidity at 51%, and the air flow at 500 μmol s^{-1}. The reference CO_2 level was set at 400 μmol mol^{-1} and the photosynthetic photon flux density (PPFD) at 800 μmol m^{-2} s^{-1} (97% light red; 3% blue). The reference CO_2 concentration reflected ambient concentrations, while the chosen PPFD reflected the photosynthetic active radiation available at mid-day in the greenhouse. Such PPFD value allowed light saturation in lettuce (i.e., 500–600 μmol m^{-2} sec^{-1}, Zhou et al., 2019), near-saturation in cucumber (600–800 μmol m^{-2} sec^{-1}, Yang et al., 2010), while sorghum remained largely undersaturated (~1800 μmol m^{-2} sec^{-1}, Tingting et al., 2010). Measurements in the Li-COR 6800 are independent of the air flow speed when the air flow surpasses values of 100–150 μmol m^{-2} sec^{-1} (Li-COR Bioscience, 2019), as in our case; the high air flow and low humidity adopted also hindered vapour condensation within the pipes of the equipment during measurement.

At the end of the trial, plants were harvested at the stage of 8 leaves in LE, 12 leaves in CU, and 7 leaves in SO (Fig. SI2) by separating the shoot from the roots to assess the dry weight (DW) biomass of the two tissues separately. This was done following oven drying for 24 h at 120 °C. Shoot DW was quantified for stem and leaves separately. Due to the prevalence of leaf over shoot biomass, the foliar-to-root biomass ratio was calculated as an index of biomass partitioning.

2.4. Statistical analysis

Statistical analysis was carried out with Statgraphics XX centurion statistical software using ANOVA and the Tuckey-Kramer test at $P \leq 0.05$. To simulate the potential of TW to improve the foliar-to-root biomass ratio as well as the separate leaf and root tissues, a Monte Carlo analysis was run using R-studio as outlined by Albert (2009).

3. Results

3.1. Absorption spectra and electro-chemical properties of treated water

The absorption coefficient (A.C.) spectrum of TW differed from that of CW mainly in the UVA-visible blue wavelength range (340–440 nm) and in the near-infrared 739–970 nm interval (Fig. 1), as supported by the Kolmorgorov Smirnov test ($P \leq 0.05$). This was clearly highlighted by the different patterns of Cumulative Relative Frequencies (CRF) for 340–440 nm and 739–970 nm wavelength intervals between TW and CW (Fig. 1), in which greater absorption peaks in TW of both regions were evident.

Indeed, the detailed A.C. distribution of TW in the 340–440 nm range highlights a decrease of frequencies at low and high A.C., along with an increase in intermediate (2.03–2.10) A.C. values (Table SI2; Fig. SI3). The trend was similar when considering the 739–970 nm wavelength range; reduced relative frequencies in the upper and lower bounds and a rise in the relative frequency of intermediate A.C. values in TW as compared to CW (Table SI3, Fig. SI3). When the A.C. values were classified in three relevant classes with similar trend, the associated wavelengths were restricted to 370–385, 394–398, and 424–432 nm classes for the UVA-Vis. region, and to 831–835, 857–870, and 881–889 nm for the near-infrared (NIR) region. In this way, TW demonstrated increased frequencies of the central classes 394–398 nm and 857–860 nm of both wavelength regions (Table 1).

The water used in this trial contained ~24 mg L^{-1} dissolved O_2 and ~100 mg L^{-1} bicarbonate, and negligible amounts of Fe, regardless of CFV treatment. As regards the electrical properties, resistance (R) and inductance (L) increased by 15% and 100% in TW in comparison to CW ($P \leq 0.05$) respectively, while pH increased by 2.3% from 7.26 to 7.43 ($P \leq 0.05$) (Table 2). The reduction in the Oxidation Reduction Potential (ORP) by 34% between TW and CW was also found to be significant.

Table 1
Relative frequency of absorption coefficients (A.C.) and absorbance classes for control (CW) and treated water (TW) and within their wavelength interval.

Wavelength	Absorbance	A.C. range	CW	TW
370–385	0.95–0.99	1.94–2.03	0.842	0.297
394–398	0.99–1.04	2.03–2.12	0.109	0.703
424–432	1.04–1.07	2.12–2.19	0.050	0
831–835	0.97–1.01	1.97–2.06	0.539	0.470
857–860	1.01–1.04	2.06–2.12	0.353	0.457
881–889	1.04–1.07	2.12–2.19	0.108	0.073

Table 2
Chemical and electrical properties (resistance R, Inductance L) (mean ± S.E; n = 3) in control (CW) and treated water (TW) (Tukey-Kramer test; $P \leq 0.05$).

Parameters	Unit	CW		TW		Significance
Dissolved O_2	mg L^{-1}	23.7	±0.31	23.9	±0.29	n.s.
ORP	mV	124	±3.99	81.8	±5.99	**
Fe^{++}	μg L^{-1}	10	±0.115	10	±0.441	n.s.
HCO_3^-	mg L^{-1}	97.8	±2.68	104	±2.02	n.s.
R	KΩ	0.13	±0.0024	0.15	±0.0076	**
L	mH	0.003	±5*10^{-11}	0.006	±0.0016	**
pH		7.26	±0.0057	7.43	±0.013	**

Significance: * at $P \leq 0.05$; ** at $P \leq 0.01$; ***$P \leq 0.001$; n.s. not significant.

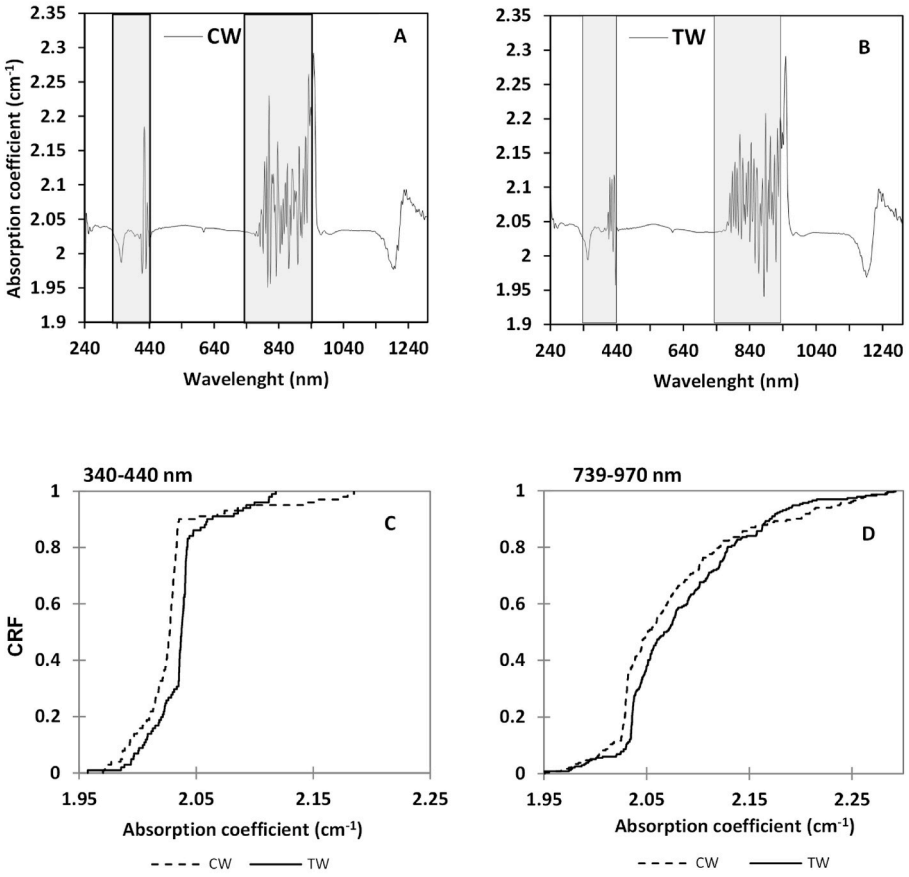

Fig. 1. Absorption coefficient of control water CW (A) and water treated with a coaxial flow variator (TW) (B) used for plant irrigation, and the respective significantly different Cumulative Relative Frequency (CRF) patterns within two wavelength intervals, i.e., 340–440 nm (C) and 739–970 nm (D). Absorption coefficient=(2.303 × Adsorbance)/d; d = sample thickness) (Kolmogorov-Smirnov test, $P \leq 0.05$).

These changes were also found in pore water at the end of the trial (Table 3) and persisted over a 12-day period, although with some variations, when the water was left unstirred on the benchtop (Fig. SI4).

3.2. Plant growth

At harvest, the plant species irrigated with TW had a different leaf, stem, and root dry biomass compared to plants irrigated with CW (Fig. 2). C3 plants, such as CU and LE, exhibited a reduction in biomass in all the three organs following irrigation with TW, although only CU roots (−27% TW vs. CW, $P < 0.05$) and LE stem (−53% TW vs. CW, $P \leq 0.05$) were significant. As such, the overall plant biomass was significantly reduced by 16% in CU, and by 23% in LE, albeit not significantly. On the contrary, in the C4 species SO, there was a significant marked increase in dry biomass in all plant organs: +34% leaves, +38% stem, and +140% roots in TW vs. CW (Fig. 2, $P \leq 0.05$). The resulting total plant biomass of SO was greatly enhanced in TW (+75% vs. CW).

When irrigated with TW, the foliar-to-root biomass ratio (Fo/R) of CU and LE increased by 17% and 14% respectively, although this was not significant, while in SO a significant decrease of Fo/R was instead observed (−42% vs. CW, $P \leq 0.05$) (Fig. 3).

Implementing the biomass data in a logistic prior function, it was possible to identify a posterior function able to describe the distribution of probability which maximizes the Fo/R ratio in each species using either CW or TW for irrigation. A Monte Carlo simulation with 10,000 cases on posterior function highlighted that CU and LE have respectively 76% and 97% probability to increase Fo/R by using TW (Fig. 4). Instead, SO showed an opposite trend with a minimal probability to increase the Fo/R ratio of just 3%. The same analysis on individual plant compartments highlighted that CU and LE had very high probability, i.e., 65% and 75% respectively, to increase the foliar biomass and low probability (35% and 25%, respectively) to increase root biomass by using TW (Fig. 4). On the contrary, SO had 22% probability to increase leaf biomass and 78% probability to increase root biomass using TW.

3.3. Photosynthesis parameters

In all the cultivated species, no significant differences were observed between TW and CW for the net CO_2 assimilation rate (A) and photosynthetic efficiency of PSII (*Fv'/Fm'*) (Fig. 5). However, a tendency for increased net assimilation and photosynthetic efficiency in LE and CU were revealed. In contrast to the improvement in plant biomass observed for SO irrigated with TW, a tendency for a decrease in net assimilation (−59% TW vs. CW $P > 0.05$) and photosynthetic efficiency (−14% TW vs. CW, $P > 0.05$) at the time of measurement (the day before harvest) was instead observed (Fig. 5).

Although having been exposed to the same radiation characteristics inside the LICOR-6800 chamber, plants irrigated with TW had significantly lower leaf temperature than those irrigated with CW. Indeed, CU, LE, and SO demonstrated leaf temperatures 1.1 °C, 0.7 °C, and 0.8 °C lower, respectively (Fig. 5). The reduced leaf temperature under TW was associated with an increase in *NPQ* in SO (+33%, $P \leq 0.05$) and LE (+32%; n.s.) compared to CW (Fig. 5), and with a reduction in *NPQ* in CU (−44%, $P \leq 0.05$).

Stomatal conductance to water vapour (*gsw*) was greater with TW vs. CW in CU (+79%), and lower in SO (−33%). No significant differences were observed in LE for *gsw* between TW and CW.

The electron transport rate (*ETR*) was 10% higher in CU irrigated with TW vs. CW, while it was 21% lower in SO. No differences were observed in LE.

Table 3
Characterization of soil pore water at the end of the experiment for resistance (R), inductance (L), and pH (mean; n = 3) in *Lactuca sativa* (LE), *Cucumis sativus* (CU), *Sorghum vulgare* (SO) irrigated with control (CW) and treated water (TW). Letters refer to comparison among species and water treatments (main effects) within the same parameter (Tukey-Kramer test, $P \leq 0.05$).

Factors	R (KΩ)	L (mH)	pH
Species			
CU	0.115[a]	0.0038[b]	7.87[a]
LE	0.174[a]	0.0051 [ab]	7.87[a]
SO	0.272[a]	0.0054[a]	7.83[a]
Treatment			
TW	0.25[a]	0.007[a]	7.91[a]
CW	0.13[b]	0.003[b]	7.82[b]
Species × Treatment	n.s.	n.s.	***

Significance: *$P \leq 0.05$; **$P \leq 0.01$; ***$P \leq 0.001$; n.s. not significant.

4. Discussion

4.1. Absorbance and electro-chemical properties of treated water

Forcing water through a CFV device allows certain electro-chemical traits of the irrigation water to be modified. Within the investigated UVA-near visible and NIR wavelength ranges the A.C. were much higher in TW compared to CW. These differences may be due to the oxidation state of the chemical species dissolved in water (Loures et al., 2013), but also to variations in the abundance of the vibrational clusters of water molecules. In this regard, TW had higher A.C. values within 394–398 nm range, which is associated with an increase in the statistical proportion of symmetric ($\nu 1$) and asymmetric ($\nu 3$) hydrogen stretching vibrations in water clusters (Pope and Fry, 1997); concurrently, higher A.C. values in the 857–860 nm range suggest a statistical reduction in bending ($\nu 2$) vibrations (Pope and Fry, 1997).

The ability of water to form hydrogen bonds depends on its molecular structure and interactions. In this way, the reduction in bending vibrations together with an increase in stretching vibrations affect the statistical distribution of molecular water vibration as highlighted by the changes in the absorption coefficient distribution (Fig. 1, SI3; Table 1, SI2, SI3). A decrease in intramolecular bending indicates that the hydrogen bonds become more rigid and that the water molecules are more firmly bonded to each other (Seki et al., 2020). It can also be argued that the increase in stretching vibrations (both $\nu 1$ and $\nu 3$) involves a lengthening, and consequently a weakening of the O–H bonds within the water molecule, while the hydrogen bonds simultaneously become stronger and on average shorter (Schmidt and Miki, 2007). This may affect the efficiency of photosystem II by improving the stability of the water molecule network with which the Oxygen Evolving Complex (OEC) of PSII is connected. Indeed, it has been demonstrated that within OEC the process of photooxidation of Mn during the S1 to S2 transition states is associated with strong hydrogen bonds of the water molecule network (Polander and Barry, 2012). Furthermore, H-bond networks connect the region of the four-Mn atom cluster of OEC to the thylakoid lumen, and when OEC works correctly the protein complexes that stabilize the Mn atoms are connected to networks of relatively complex water molecules held together by numerous hydrogen bonds. On the contrary, in the case of inefficient OEC functioning, the water protein network appears to be composed of 5 times fewer water molecules containing few hydrogen bonds (Guerra et al., 2018).

Based on the electrical measurements in this study, it is expected that water treated with the CFV device can enter the OEC supply channel with a lower atomic displacement parameter thanks to stronger hydrogen bonds and cohesion among molecules. Treated water can therefore be transported more easily compared to untreated water, thus facilitating proton relay processes (Hussein et al., 2021). Treated water could also allow a better coordination of the movement of the water network with the amino acid residues present in the OEC, which is fundamental to spatially control the transport of water for photolysis (Hussein et al., 2021). Furthermore, the weakening of the O–H bond as a result of the strengthening of the hydrogen bonds may facilitate the deprotonation of water after it has bonded to the Mn and Ca atoms of the OEC. It has also been demonstrated that well ordered water structures

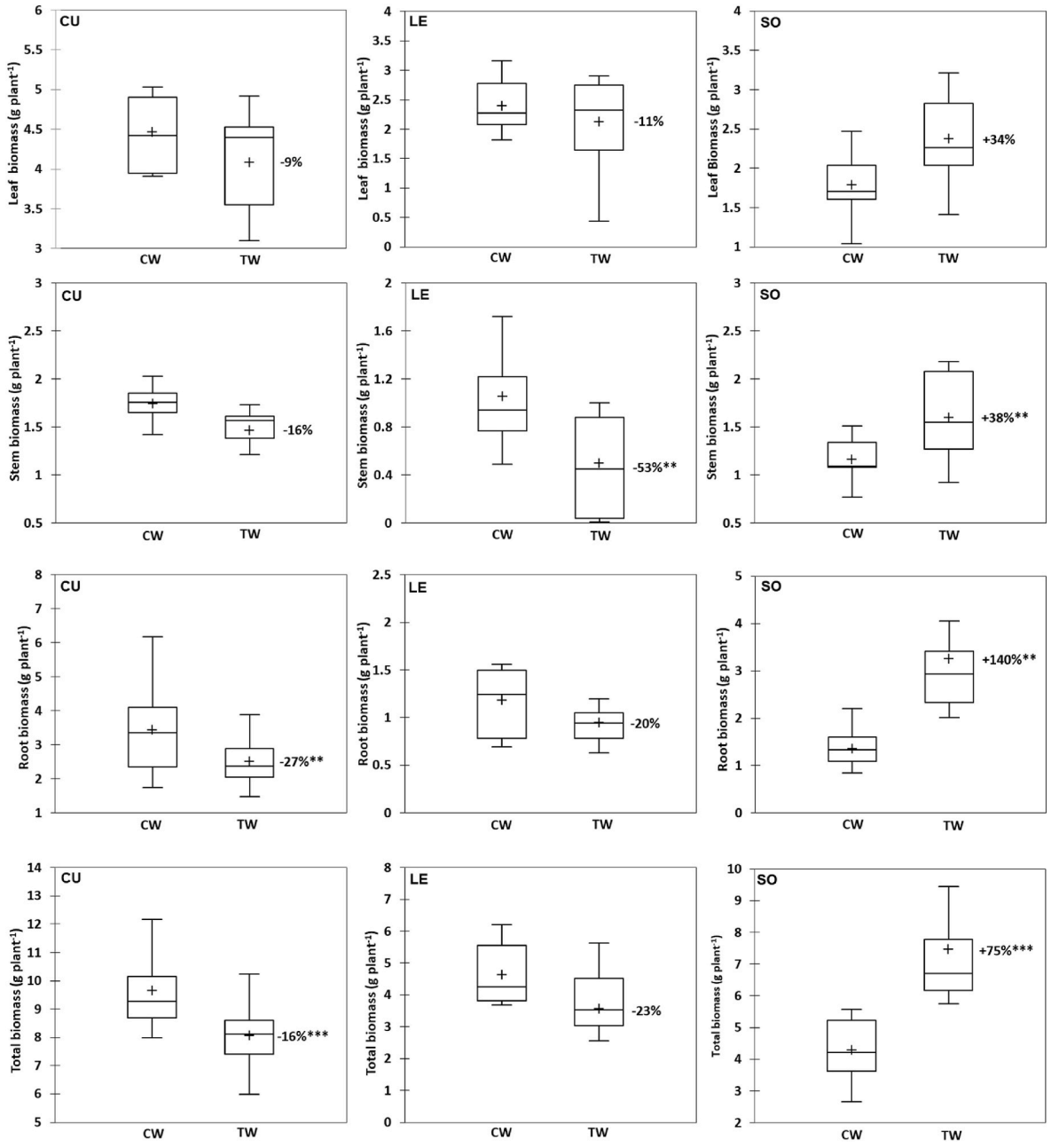

Fig. 2. Leaf, stem, root, and total plant dry biomass in *Cucumis sativus* (CU), *Lactuca sativa* (LE), and *Sorghum vulgare* (SO) irrigated with treated (TW) and control water (CW). With their shape, the box and whisker plots indicate from top to bottom: the maximum value, the upper quartile (Q3), the median (crossing the interquartile range), the lower quartile (Q1), and the minimum value. The cross represents the mean of the distribution.

with stronger hydrogen bonds facilitate the Grotthuss-like proton transfer from the OEC to the thylakoid lumen and protects/stabilizes the OEC from small molecule reductants (Russell and Vinyard, 2024).

The motion of water inside the CFV device causes a twist in the fluid flow, thus promoting mixing and collision of water molecules, increasing the chances of forming new hydrogen bonds. As O_2 and HCO_3^- contents were found to be similar between TW and CW (Table 2), no significant mixing with atmospheric gases such as O_2 and CO_2 occur within the CFV device, suggesting that the formation of bubbles and nano-bubbles during the water flow in the CFV did not take place.

Although most of the chemical characteristics of irrigation water in this study did not change, a reduction of ORP (Table 2) as a result of water treatment could easily be assessed from our preliminary observations regardless of the origin and/or quality of water. This means that TW had lower levels of ROS, possibly facilitated by the electron exchange from free radicals to the metallic surface of the CFV made of iron and copper. This agrees with the more alkaline pH measured in TW (Table 2). Greater pH can furtherly facilitate the formation of hydrogen bonds due to the increased abundance of hydroxyl ions, which have greater attack surface for hydrogen bonding. It is likely that ROS species such as super oxide O_2^- can react with Fe atoms or with Fe oxide that forms on the internal surface of the CFV device. This would result in reduction reactions lowering the ORP (Ivanović-Burmazović, 2008; Ivanović-Burmazović and van Eldik, 2008). As an alternative, normal corrosion of Fe in presence of oxygen and water can lead to the formation of oxidized species of Fe and OH^- ions with a consequent increase in pH (Slabaugh, 1974). In turn, the rise in pH is very probably responsible for the increase in electrical resistance R measured in TW. Commonly pH increases can be associated with improvements in electrical conductivity of water solutions (Ratnayake et al., 2017). Greater conductivity

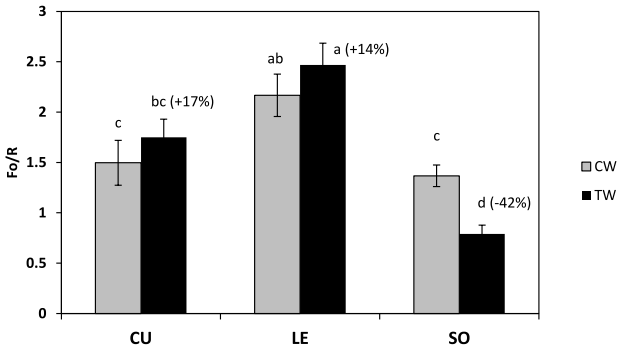

Fig. 3. Foliar-to-root dry biomass ratio (Fo/R) (mean ± S.E.; n = 9) in *Cucumis sativus* (CU), *Lactuca sativa* (LE), and *Sorghum vulgare* (SO) irrigated with control (CW) and treated water (TW). Different letters indicate significant differences for multiple comparisons (Tuckey-Kramer test; $P \leq 0.05$).

increases the dispersion of electrical current from the solenoid used for measurements which can be observed as increases in resistance (Table 2).

As highlighted by Hamauzu et al. (2014), changes in ORP are reflected in some of the electrical properties of water. In this trial, the R and L of TW was greater than that of CW. The greater inductance L can be related to an enhanced permeability of water to the magnetic flux, ϕ. The magnetic flux is thereby less contrasted by other magnetic resultants coming from molecular motion, and as such, the self-induction coefficient of the measurement circuit results higher compared to CW.

The question which arises is how long these electro-chemical changes of TW can persist. Although not conclusive, and not representative of the medium to which the water is applied during irrigation, benchtop measurements indicate that the changes in the electrical properties of water can, to some extent, persist at least over 10–12 days, and likely longer (Fig. SI4). This aspect in this study may be of little importance however, as the water was treated every time immediately before irrigating the plants during the trial.

The hydrogen bonds in water plays a crucial role in water's ability to dissolve and interact with many substances. Hydrogen bonds allow water molecules to form hydration shells around ions and polar molecules, facilitating their dissolution and chemical reactions (Laage et al., 2017). On the contrary, when water forms few hydrogen bonds, it becomes less effective at solvating and at stabilizing charged and polar molecules, thus resulting less reactive. Additionally, hydrogen bonds in water affects the reactivity of functional groups in biomolecules, such as amino and hydroxyl groups in proteins and nucleic acids (Barciszewski et al., 1999; Sterpone et al., 2010). Thus, a decrease in the number of hydrogen bonds can impact the conformation and stability of these biomolecules, potentially affecting their reactivity and interactions with other molecules. As hydrogen bonding in water involves the electrostatic interaction between the partially positive hydrogen atom of one water molecule and the partially negative oxygen atom of another water molecule, TW, with reduced ORP, and increased pH, R, and L, is expected to better promote biological processes in comparison to CW.

4.2. Photosynthesis and growth in test plant species under irrigation with treated water

In the C3 species LE and CU, a trend of improved net assimilation rate and photosynthetic efficiency under TW was evident, although with

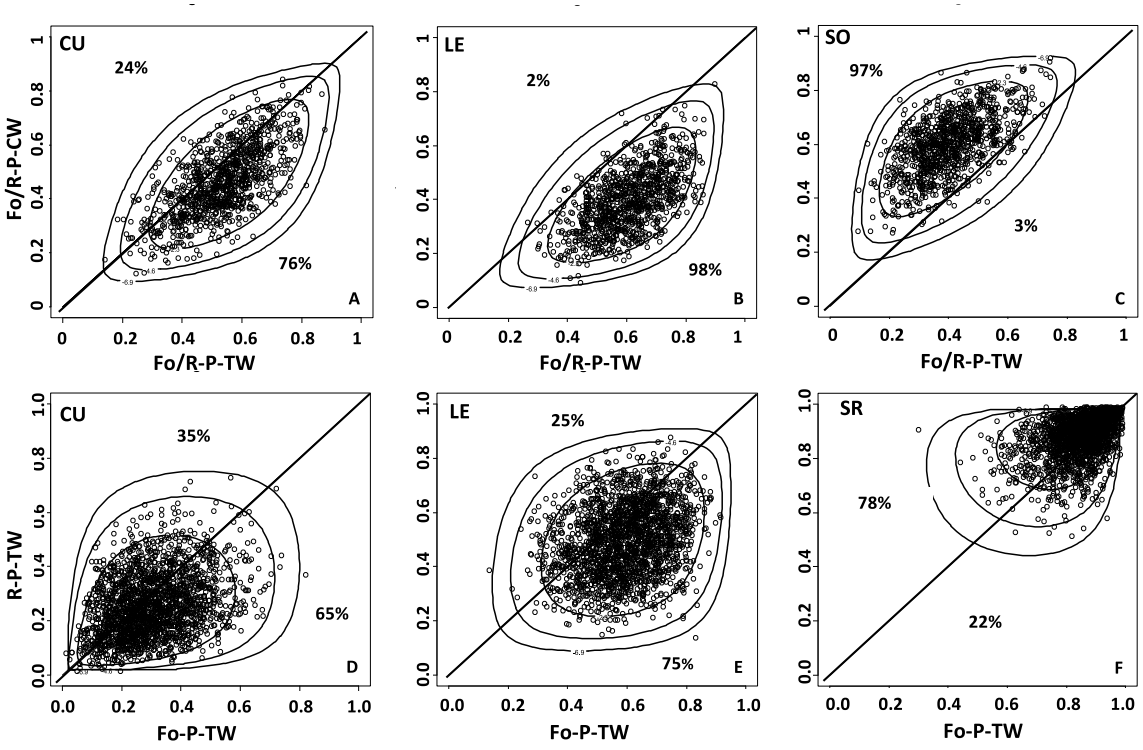

Fig. 4. Contour plots of Monte Carlo posterior distribution analysis with 10,000 cases for the foliar-to-root biomass ratio (Fo/R) (A–C), and foliar and root biomasses (D–F) in *Cucumis sativus* (CU), *Lactuca sativa* (LE), and *Sorghum vulgare* (SO). Contour lines drawn at 10% (outer), 1%, and 0.1% (inner) of model height. Howard-simulated random samples from this distribution overlaps contour plot (Howard function, parameter $\delta = 0.05$). Fo/R-P-TW: probability to maximize Fo/R using treated water (TW); Fo/R-P-CW: probability to maximize Fo/R using control water (CW); Fo-P-TW: probability to maximize foliar biomass (Fo) using treated water (TW); R-P-TW: probability to maximize root biomass (R) using (TW). The percentages indicate the Kernel density separation with respect to the graph diagonal.

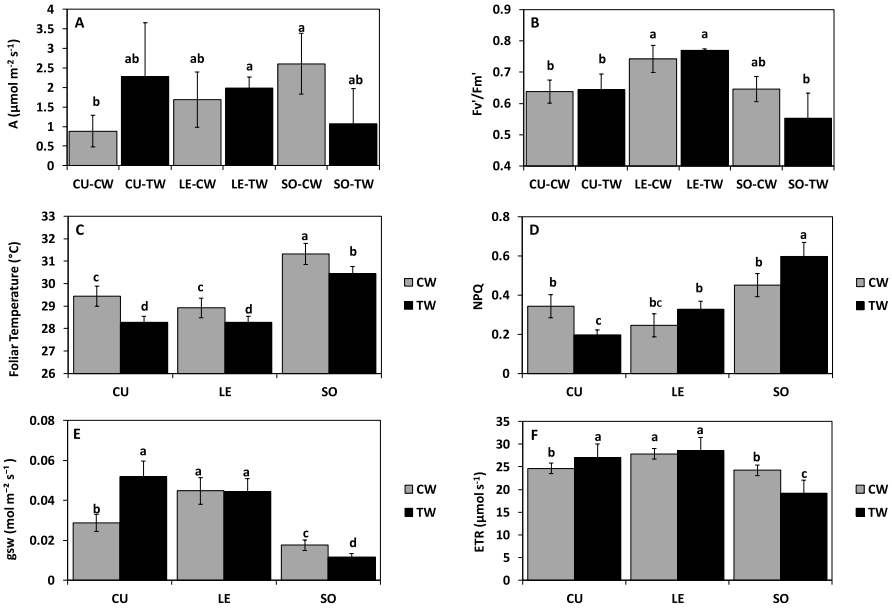

Fig. 5. Species × treatment (mean ± SE; n = 9) interaction concerning Net Assimilation Rate (A), Photosynthesis Efficiency (Fv'/Fm') (B) leaf temperature (C), non-photochemical quenching (*NPQ*) (D), stomatal conductance (*gsw*) (E), and electron transport rate (*ETR*) (F) in *Cucumis sativus* (CU), *Lactuca sativa* (LE), and *Sorghum vulgare* (SO) irrigated with control (CW) and treated water (TW). Letters for multiple comparisons (Tuckey-Kramer test, $P \leq 0.05$).

some variations (Fig. 5). Light conditions permitted CU to be tested under near light saturation of PSII and the effect of TW corresponds to a greater physiological efficiency model, with an increase in stomatal conductance and electron transport rate, and a decrease in NPQ. Instead, the light conditions oversaturated the photosynthetic capacity of LE likely inducing a significant increase in NPQ due to excess radiation. In LE, stomatal conductance and ETR remain unchanged. In SO, TW seemed to impede the photosynthetic metabolism, causing a decrease in stomatal conductance and ETR, and an increase in NPQ, which is in contrast with the marked biomass increase observed at the end of the trial. Actually, the photosynthesis data of SO depict a condition in which plants irrigated with TW anticipated their growth by at least one week. The investigated leaf of SO-CW was thus younger compared to SO-TW and was therefore still actively growing and possessing a more active photosynthetic metabolism (Allen Jr. et al., 2011).

The decrease in foliar temperature across all species when irrigated with TW, is an important result and is probably due to a greater leaf water content, which is generally associated with an enhanced leaf metabolism (Wang et al., 2022). We did not measure the leaf water content in this trial, but water works as a thermal flywheel by delaying thermal increases in open environments or, in this case, within the analysis chamber of the Li-COR equipment. The decrease in leaf temperature was associated with a reduction of NPQ in CU, but this was not a rule in the current trial. Indeed, Herdean et al. (2023) found an inverted relationship between leaf temperature and NPQ if the ΔpH across the thylakoid membrane is altered. TW, with its greater pH, may therefore have induced an immediate NPQ increase in LE and SO plants.

Many of these results suggest that the impact of water treatment was compatible with the effect of water having a greater number of hydrogen bonds, as discussed above, and thereby promoting efficient biochemical reactions related to photosynthesis. However, this was unexpectedly translated into plant biomass decreases in both C3 plant species CU and LE, which involved both shoot and root compartments, while a marked biomass increase was recorded in the C4 species SO, particularly at root level (Fig. 2). Root and total plant weight reductions were significant in CU, and leaf biomass in LE, leading to an increase in the shoot-to-root ratio, here calculated using the foliar biomass as the major above-ground component (Fig. 3). While microscopy investigations will be necessary to ascertain whether TW can increase the accumulation of low-density aquifer parenchyma over sclerotized tissues with thicken cell walls (Le Gall et al., 2015), the Monte Carlo analysis demonstrated that the increased shoot-to-root biomass ratio of CU and LE is more likely the result of greater root than shoot growth reduction (Fig. 4). Similar results were also obtained by Hamauzu et al. (2014) using irrigation water with modified ORP induced via electric current flow. Based on the above- and below-ground functional equilibrium in plants (van Noordwijk and de Williogen, 1987), such a result would suggest more favourable soil conditions with TW irrigation than CW irrigation.

The C4 photosynthetic pathway involves the assimilation of CO_2 by phosphoenolpyruvate carboxylase (PEPC) and subsequent decarboxylation of the C4 acids. The involved enzymes are affected by low water availability in tissues thus limiting photosynthesis (Carmo-Silva et al., 2008); therefore, better tissue hydration expected under TW could explain the high biomass production in SO. It can also be hypothesized that water with a greater number of hydrogen bonds can more effectively transport malic acid from the mesophyll cells to the bundle sheath cells through cell membranes. This could be explained by an ameliorated stability of membrane proteins deriving from the breaking and reformation of hydrogen bonds which facilitate conformational changes in protein membrane channels (Hildebrand et al., 2008).

TW allowed a notable increase in SO biomass (>30% at shoot, and >140% at root level), which seemingly favoured a rapid advancement of the plant cycle with respect to CW, and contributed to the shoot-to-root biomass decrease within the resource-limiting environment of the pots. In this regard, the photosynthetic response in SO confirms literature observations (Nath et al., 2013; Zhang et al., 2019; Lu et al., 2021) on *ETR* and *gsw* decreases with advancement of the plant cycle, as occurred under TW in this trial. Such findings advocate for future investigations into the effect on photosynthesis to be carried out as early as possible, when growth differences between TW- and CW-treated plants do not diverge excessively.

5. Conclusions

Inducing water turbulence with a CFV can promote electro-chemical modifications of water, hereunder particularly modifications related to

alkalinization and reductions in ORP. This produces a sort of functionalized water with possibly an augmented proportion of stretching vibrational clusters and number of hydrogen bonds among water molecules. Such TW is therefore expected to interact differently with biochemical processes related to photosynthesis. Net assimilation demonstrated an increased trend in both LE and CU. The trend was instead contrary for SO likely due to the timing of measurements coinciding with the descending phase of the assimilation-leaf age curve response. A reduction in leaf temperature across all species suggests plants to be more hydrated and therefore experience less heat stress when irrigated with TW. This was efficiently translated into improved biomass yield only in SO however. TW thus has the potential to improve plant adaptation to external conditions.

Certain photosynthetic parameters specific to the species were improved. Given the restricted number of species here investigated, at this time it is difficult to predict a contrasting C3 vs. C4 response model to TW. Changes in the shoot-to-root biomass, which was observed to both increase and decrease, demonstrate possible interesting application in crop cultivation, particularly in the controlled environment of a greenhouse.

In this preliminary trial, the photosynthetic efficiency was investigated as the potential major driver of plant growth. However, much remains to be elucidated regarding other physiological processes, plant species, and growth stages (up to maturity). Further investigation necessitate insights into soil water potential and nutrient dissolution/bio-availability allowing for full exploitation of TW in agricultural settings.

Funding

This research received no external funding.

CRediT authorship contribution statement

Giuseppe Barion: Writing – review & editing, Writing – original draft, Methodology, Investigation, Data curation. **Camilla Canal:** Investigation, Data curation. **Anna Panozzo:** Writing – review & editing. **Selina Sterup Moore:** Writing – review & editing. **Simone Piotto:** Investigation. **Teofilo Vamerali:** Writing – review & editing, Supervision, Resources, Project administration, Methodology, Conceptualization.

Declaration of competing interest

The authors declare that they have no known competing financial interests or personal relationships that could have appeared to influence the work reported in this paper.

Data availability

Data will be made available on request.

Acknowledgments

The authors wish to thank Adriano Massignan for helping with data collection.

Appendix A. Supplementary data

Supplementary data to this article can be found online at https://doi.org/10.1016/j.plaphy.2024.108780.

References

Albert, J., 2009. Bayesian Computation with R. Springer Science & Business Media, p. 300.

Allen, Jr L.H., Kakani, V.G., Vu, J.C., Boote, K.J., 2011. Elevated CO_2 increases water use efficiency by sustaining photosynthesis of water-limited maize and sorghum. J. Plant Physiol. 168 (16), 1909–1918.

Barciszewski, J., Jurczak, J., Porowski, S., Specht, T., Erdmann, V.A., 1999. The role of water structure in conformational changes of nucleic acids in ambient and high-pressure conditions. Eur. J. Biochem. 260, 293–307.

Bernath, P.F., 2002. The spectroscopy of water vapour: experiment, theory and applications. Phys. Chem. Chem. Phys. 4, 1501–1509.

Blatt, M.R., Chaumont, F., Farquhar, G., 2014. Focus on water. Plant Physiol. 164, 1553–1555.

Carmo-Silva, A.E., Bernardes da Silva, A., Keys, A.J., Parry, M.A., Arrabaca, M.C., 2008. The activities of PEP carboxylase and the C4 acid decarboxylases are little changed by drought stress in three C4 grasses of different subtypes. Photosynth. Res. 97, 223–233.

Cooper, M.M., Stowe, R.L., Crandell, O.M., Klymkowsky, M.W., 2019. Organic chemistry, life, the universe and everything (OCLUE): a transformed organic chemistry curriculum. J. Chem. Educ. 96, 1858–1872.

Eisenberg, D., Kauzmann, W., 2005. The Structure and Properties of Water. Oxford University Press, p. 308.

Guerra, F., Siemers, M., Mielack, C., Bondar, A.N., 2018. Dynamics of long-distance hydrogen-bond networks in photosystem II. J. Phys. Chem. B 122 (17), 4625–4641.

Hamauzu, Y., Ishikawa, K., Morisawa, S., 2014. Effects of deoxidized nutrient solution on growth of komatsuna (*Brassica rapa* var. *perviridis*) plants. Environ. Control Biol. 52, 107–111.

Herdean, A., Hall, C., Hughes, D.J., Kuzhiumparambil, U., Diocaretz, B.C., Ralph, P.J., 2023. Temperature mapping of non-photochemical quenching in *Chlorella vulgaris*. Photosynth. Res. 155, 191–202.

Hildebrand, P.W., Günther, S., Goede, A., Forrest, L., Frömmel, C., Preissner, R., 2008. Hydrogen-bonding and packing features of membrane proteins: functional implications. Biophys. J. 94, 1945–1953.

Hopkins, W.G., Hüner, N.P.A., 2004. Introduction to Plant Physiology, third ed. John Wiley & Sons, Inc, Hoboken, p. 580.

Hussein, R., Ibrahim, M., Bhowmick, A., Simon, P.S., Chatterjee, R., Lassalle, L., Doyle, M., Bogacz, I., Kim, I., Cheah, M.H., Gul, S., de Lichtenberg, C., Chernev, P., Pham, C.C., Young, I.D., Carbajo, S., Fuller, F.D., Alonso-Mori, R., Batyuk, A., Sutherlin, K.D., Brewster, A.S., Bolotovsky, R., Mendez, D., Holton, J.M., Moriarty, N.W., Adams, P.D., Bergmann, U., Sauter, N.K., Dobbek, H., Messinger, J., Zouni, A., Kern, J., Yachandra, V.K., Yano, J., 2021. Structural dynamics in the water and proton channels of photosystem II during the S2 to S3 transition. Nat. Commun. 12, 6531.

Ivanović-Burmazović, I., 2008. Catalytic dismutation vs. reversible binding of superoxide. Adv. Inorg. Chem. 60, 59–100.

Ivanović-Burmazovića, I., Eldika van, R., 2008. Metal complex-assisted activation of small molecules. From NO to superoxide and peroxides. Dalton Trans. 39, 5259–5275.

Laage, D., Elsaesser, T., Hynes, J.T., 2017. Water dynamics in the hydration shells of biomolecules. Chem. Rev. 117, 10694–10725.

Le Gall, H., Philippe, F., Domon, J.M., Gillet, F., Pelloux, J., Rayon, C., 2015. Cell wall metabolism in response to abiotic stress. Plants 4, 112.

Li-COR Bioscience, 2019. Making one-sided leaf measurements. Li-COR Application note 18444, 1–4.

Loures, C.C.A., Alcântara, M.A.K., Izário, Filho, H.J., Teixeira, A.C.S.C., Silva, F.T., Paiva, T.C., B. Samanamud, G.R.L., 2013. Advanced oxidative degradation processes: fundamentals and applications. Int. Rev. Chem. Eng. 5, 2035-1755.

Lu, Y., Xu, J., Liu, X., 2021. A process-based coupled model of stomatal conductance–photosynthesis–transpiration during leaf ontogeny for water-saving irrigated rice. Photosynth. Res. 147, 145–160.

Maréchal, Y., 2011. The molecular structure of liquid water delivered by absorption spectroscopy in the whole ir IR region completed with thermodynamics data. J. Mol. Struct. 1004, 146–155.

Mecklenburg, S., Drusch, M., Kerr, Y.H., Font, J., Martin-Neira, M., Delwart, S., Buenadicha, G., Reul, N., Daganzo-Eusebio, E., Oliva, R., 2012. ESA's soil moisture and ocean salinity mission: mission performance and operations. IEEE Trans. Geosci. Rem. Sens. 50, 1354–1366.

Nath, K., Phee, B.K., Jeong, S., Lee, S.Y., Tateno, Y., Allakhverdiev, S.I., Nam, H.G., 2013. Age-dependent changes in the functions and compositions of photosynthetic complexes in the thylakoid membranes of Arabidopsis thaliana. Photosynth. Res. 117, 547–556.

Piatkowski, L., Bakker, H., 2011. Vibrational dynamics of the bending mode of water interacting with ions. J. Chem. Phys. 135, 214509.

Polander, B.C., Barry, B.A., 2012. A hydrogen-bonding network plays a catalytic role in photosynthetic oxygen evolution. Proc. Natl. Acad. Sci. USA 109 (16), 6112–6117.

Pope, R.M., Fry, E.S., 1997. Absorption spectrum (380–700 nm) of pure water. ii. Integrating cavity measurements. Appl. Opt. 36, 8710–8723.

Ratnayake, A.S., Dushyantha, N., De Silva, N., Somasiri, H.P., Jayasekara, N.N., Weththasinghe, S.M., Vijitha, A.V.P., Ratnayake, N.P., 2017. Sediment and physicochemical characteristics in Madu-Ganga Estuary, southwest Sri Lanka. J. Geol. Soc. Sri Lanka 18 (2), 43–52.

Rice, E.W., Bridgewater, L., 2012. Standard methods for the examination of water and wastewater. In: American Public Health Association, vol. 10. American Public Health Association, Washington, DC, p. 1360.

Russell, B.P., Vinyard, D.J., 2024. Conformational changes in a Photosystem II hydrogen bond network stabilize the oxygen-evolving complex. BBA-Bioenergetics 1865 (1), 149020.

Ruud, K., Jonsson, D., Taylor, P.R., 2000. Vibrational effects on electric and magnetic susceptibilities: application to the properties of the water molecule. Phys. Chem. Chem. Phys. 2, 2161–2171.
Sajovic, I., 2004. Patent SI 21511 (A) - 2004-12-31. Accessory for Generating Turbulence in Plumbing. European Patent Organisation. Bob-van-Benthem-Platz 1 80469 Munich, DE.
Schmidt, D.A., Miki, K., 2007. Structural correlations in liquid water: a new interpretation of IR spectroscopy. J. Phys. Chem. A 111, 10119–10122.
Seki, T., Chiang, K.Y., Yu, C.C., Yu, X., Okuno, M., Hunger, J., Nagata, Y., Bonn, M., 2020. The bending mode of water: a powerful probe for hydrogen bond structure of aqueous systems. J. Phys. Chem. Lett. 11, 8459–8469.
Slabaugh, W.H., 1974. Corrosion. J. Chem. Educ. 51 (4), 218–220.
Sterpone, F., Stirnemann, G., Hynes, J.T., Laage, D., 2010. Water hydrogen-bond dynamics around amino acids: the key role of hydrophilic hydrogen-bond acceptor groups. J. Phys. Chem. B 114, 2083–2089.
Tennyson, J., Bernath, P.F., Brown, L.R., Campargue, A., Csasz, A.G., Daumont, L., Gamache, R.R., Hodges, J.T., Naumenko, O.V., Polyansky, O.L., 2014. A database of water transitions from experiment and theory (IUPAC technical report). Pure Appl. Chem. 86, 71–83.
Tingting, X., Peixi, S., Lishan, S., 2010. Photosynthetic characteristics and water use efficiency of sweet sorghum under different watering regimes. Pakistan J. Bot. 42 (6), 3981–3994.
van Noordwijk, M., de Willigen, P., 1987. Agricultural concepts of roots: from morphogenetic to functional equilibrium between root and shoot growth. Neth. J. Agric. Sci. 35, 487–496.
Wang, Z., Huang, H., Wang, H., Peñuelas, J., Sardans, J.Niinemets, Wright, I.J., 2022. Leaf water content contributes to global leaf trait relationships. Nat. Commun. 13 (1), 5525.
Walrafen, G., Pugh, E., 2004. Raman combinations and stretching overtones from water, heavy water, and NaCl in water at shifts to ca. 7000 cm^{-1}. J. Solut. Chem. 33, 81–97.
Wozniak, B., Dera, J., 2007. Light Absorption in Sea Water, vol. 33. Springer, p. 394.
Yang, X., Wang, X., Wei, M., 2010. Response of photosynthesis in the leaves of cucumber seedlings to light intensity and CO_2 concentration under nitrate stress. Turk. J. Bot. 34 (4), 303–310.
Zhang, F., Zhu, K., Wang, Y.Q., Zhang, Z.P., Lu, F., Yu, H.Q., Zou, J.Q., 2019. Changes in photosynthetic and chlorophyll fluorescence characteristics of sorghum under drought and waterlogging stress. Photosynthetica 57, 1156–1164.
Zhou, J., Li, P., Wang, J., Fu, W., 2019. Growth, photosynthesis, and nutrient uptake at different light intensities and temperatures in lettuce. Hortscience 54 (11), 1925–1933.